

Journal of Materials Chemistry C

Accepted Manuscript



This is an *Accepted Manuscript*, which has been through the Royal Society of Chemistry peer review process and has been accepted for publication.

Accepted Manuscripts are published online shortly after acceptance, before technical editing, formatting and proof reading. Using this free service, authors can make their results available to the community, in citable form, before we publish the edited article. We will replace this *Accepted Manuscript* with the edited and formatted *Advance Article* as soon as it is available.

You can find more information about *Accepted Manuscripts* in the [Information for Authors](#).

Please note that technical editing may introduce minor changes to the text and/or graphics, which may alter content. The journal's standard [Terms & Conditions](#) and the [Ethical guidelines](#) still apply. In no event shall the Royal Society of Chemistry be held responsible for any errors or omissions in this *Accepted Manuscript* or any consequences arising from the use of any information it contains.

Cite this: DOI: 10.1039/c0xx00000x

www.rsc.org/xxxxxx

ARTICLE TYPE

One-Pot Synthesis of Carbon Nanodots for Fluorescence Turn-on Detection of Ag⁺ based on the Ag⁺-Induced Enhancement of Fluorescence

Xiaohui Gao,^{a,b} Yizhong Lu,^{a,b} Ruizhong Zhang,^{a,b} Shuijian He,^{a,b} Jian Ju,^a Minmin Liu,^{a,b} Lei Li,^a and Wei Chen^{*a}

Received (in XXX, XXX) Xth XXXXXXXXX 20XX, Accepted Xth XXXXXXXXX 20XX

DOI: 10.1039/b000000x

Carbon quantum dots are promising fluorescence probes with applications in metal ions detection, biosensing and bioimaging etc. In this study, water-soluble carbon nanodots are synthesized through a simple one-step heat treatment of ethyl glycol solution. In the present preparation, the C-dots may be formed through the hydration, crosslinking and carbonization processes. The synthesized C-dots show green luminescent emission under ultraviolet excitation, which can be used for the detection of Ag⁺ ions. Interestingly, different from the usual quenching effects of metal ions on the fluorescence of C-dots, Ag⁺ exhibited an enhancement effect on the photoluminescence of C-dots, which can be attributed to the reduction of Ag⁺ to silver nanoclusters (Ag⁰) on the surface of carbon dots. Based on the linear relationship between fluorescence intensity and concentration of Ag⁺ ions, the prepared C-dots can be used to sensitive and selective detection of silver ions in environmental water with a limit of detection of 320 nM and a linear range of 0-90 μM.

1. Introduction

With the rapid development of industry, heavy metal ions have become one primary class of pollutants in our environment, which could be a serious threat to our health.¹ As a type of noble metal, silver is very important to human beings due to its charming properties and multi-functions which make it has wide applications in our daily life, such as decoration and materials for curing the diseases, e.g. rheumatism. On the other hand, silver is also largely used in electronic, photographic and imaging industries.² However, silver ions have been classified to one of the most poisonous heavy metal ions.³ Thus, determination of the concentration of silver (I) ions in freshwater or seawater is necessary for ensuring the non-polluted environment that we live in and no harmful to our health. Although many modern instrumentally analytical techniques such as atomic absorption/emission spectroscopy and inductively coupled plasma mass spectroscopy, have been applied to the analyzing trace content of Ag⁺ in water,⁴ these techniques require complicated instruments and/or sample preparation processes, resulting in the limitation of their application. On the other hand, compared to sensors for detection of other metal ions, the existing fluorescence probes for Ag⁺ detection are relatively scarce.⁵⁻⁷ Therefore, more simple and rapid methods for the precise determination of silver concentration are still needed.

Fluorescent nanomaterials have been investigated by chemists

and biologists for a long time because these materials could be used in different areas, such as chemical sensors, biosensors and bioimaging etc.⁸⁻¹² Among the studied fluorescent probes, carbon nanodots (C-dots) have attracted increasing attention in recent years due to their good stability, high biocompatibility and low cytotoxicity compared to semiconductor quantum dots and organic fluorophores.¹³⁻¹⁶ Up to now, there have developed various methods for the preparation of fluorescent C-dots. For example, by taking advantage of a microfluidic system Alonso-Chamarro and co-workers prepared C-dots for application in optical pH sensors.¹⁷ Recently, Zhang et al. presented an economical and green synthesis method for synthesizing fluorescent C-dots and their application for Hg²⁺ detection based on the Hg²⁺-induced fluorescence quenching.¹⁸ In another study, high photoluminescent C-dots were synthesized by Zhu et al, and the fluorescent carbon particles can be utilized for the detection of Fe³⁺ in biosystems.¹⁹ Additionally, C-dots have also been used as fluorescent probes for sensing other metal ions.^{20,21}

Except for the carbon nanodots, fluorescent heteroatom-doped C-dots and graphene quantum dots have also been prepared and extensively studied as sensing probes for metal ions detection.²²⁻²⁵ For example, our group synthesized N-doped carbon dots for detection of Hg²⁺ and graphene quantum dots for recognition of Fe³⁺.^{18, 26} It should be pointed out that in these studies, the sensitive detection of metal ions was realized based on fluorescence quenching by metal ions. Meanwhile, to the best of our knowledge, the carbon dots-based fluorescence sensing for

the detection of Ag⁺ ions is scarce. In a recent study, Algarra et al.²⁷ reported the functionalization of luminescent C-dots and their application as effective sensing platform for Ag⁺ ions, on the basis of quenching effect of Ag⁺ on the fluorescence of C-dots.

Herein, we present a one-step and simple method to synthesize fluorescent carbon dots directly from ethyl glycol at high temperature under the protection of inert gas. The obtained C-dots exhibited green luminescence. Interestingly, different from the previous observation of quenched fluorescence by metal ions, the fluorescence intensity of the C-dots can be enhanced upon addition of silver ions. Based on the linear relationship between the enhanced fluorescence intensity and Ag⁺ concentration, the selective, sensitive detection of Ag⁺ ions was achieved with the prepared C-dots. Moreover, the prepared carbon nanodots can also be applied to the determination of Ag⁺ concentration in environmental lake water. The possible mechanisms of the formation of C-dots and the Ag⁺-induced fluorescence enhancement are proposed.

2. Experimental Section

2.1 Materials

Ethyl glycol (C₂H₆O₂), sodium hydroxide (NaOH), hydrochloric acid (HCl), nitric acid (HNO₃), sulfuric acid (H₂SO₄), sodium dihydrogenphosphate dehydrate (NaH₂PO₄·2H₂O), and di-sodium hydrogen phosphate dodecahydrate (Na₂HPO₄·12H₂O) were purchased from Beijing Chemical Reagent. Quinine sulfate was obtained from Sigma-Aldrich. Standard stock (10 mM) of metal ions (Hg²⁺, Ca²⁺, Fe³⁺, Na⁺, Cu²⁺, K⁺, Ni²⁺, Co²⁺, Pb²⁺, Ag⁺, Mn²⁺, Mg²⁺, Zn²⁺, Cd²⁺) were prepared with ultrapure water from the respective metal salts (NaCl, KCl, CuCl₂·H₂O, ZnCl₂, CaCl₂, FeCl₃·6H₂O, AgNO₃, MgSO₄, Hg(NO₃)₂·1/2H₂O, MnCl₂, NiCl₂·6H₂O, Pb(NO₃)₂, CoCl₂·6H₂O, Cd(CHCOO)₂·H₂O). All the reagents are of analytical reagent grade and used as received. And all the aqueous solutions were prepared with ultrapure water supplied by a Water Purified Nanopure water system (18.3 MΩ cm).

2.2 Synthesis of carbon dots

C-dots were synthesized directly from an ordinary dihydric alcohol, i.e. ethyl glycol by a simple heating treatment. In a typical reaction, 20 mg of sodium hydroxide was added to 2 ml of ethyl glycol in the round-bottomed flask and this mixture was sonicated for 5 min at room temperature. After the solid was dissolved completely, the reaction was left stirring at 25 °C for 30 min. Then, the solution was heated at 185 °C for 30 min under the protection of nitrogen atmosphere. After 30 min, the color of the solution changed from colorless to light and then deep yellow gradually, which indicates the formation of C-dots. After the solution was cooled down to room temperature, the product was separated and dried under vacuum to get a yellow solid of C-dots for further characterization. Additional experiments were performed to study the effect of solution pH on the fluorescence of the prepared C-dots. Such experiments were carried out with the same procedure described above except for adding HCl (1 M, 1.5 ml) or different amounts of sodium hydroxide (0 mg, 10 mg) to the reaction solution.

2.3 Material characterization

UV-Vis spectra were recorded on UV-3000PC Spectrophotometer (Shanghai Manada Instruments Co.,Ltd). Photoluminescence spectra (PL) were recorded on a Perkin-Elmer LS-55 Luminescence Spectrometer (Perkin-Elmer Instruments U.K). X-ray photoelectron spectroscopy (XPS) measurements were performed by using AVG Thermo ESCALAB250 spectrometer (VG Scientific) operated at 120 W. Fourier-transformed infrared spectroscopy (FTIR) study was conducted with a vertex 70FTIR (KBr wafer technique). The size and morphology of C-dots were examined by using a Hitachi H-600 transmission electron microscope (TEM) operated at 100 kV.

2.4 Fluorescence detection of Ag⁺ ions

In a typical run, 370 μL of the original C-dots solution was diluted to 3 mL by nanopure water. AgNO₃ solutions were prepared from the stock solution (10 mM) with water. Different volumes of Ag⁺ solution were added into the C-dots solution and the corresponding fluorescence spectra were recorded at room temperature after one minute of mixing. To examine the selectivity of the prepared C-dots for Ag⁺ detection, 6 μL, 10 mM of other different metal cations (Hg²⁺, Ca²⁺, Fe³⁺, Na⁺, Cu²⁺, K⁺, Ni²⁺, Co²⁺, Pb²⁺, Ag⁺, Mn²⁺, Mg²⁺, Zn²⁺, Cd²⁺) were also added to the C-dots solution to study their effects on the fluorescence of C-dots. In addition, detection of Ag⁺ in a real water sample was performed by using the lake water from South Lake of Changchun, Jilin province with the similar experimental procedures described above.

2.5 Quantum yield (QY) measurements

The measuring experiment of quantum yield (QY) of the prepared C-dots was conducted according to the established procedure. In the measurement, quinine sulfate in 0.1 M H₂SO₄ (QY = 0.54 in water) was used as standard sample. The fluorescence quantum yield value of the C-dots could be calculated on the basis of the following equation:

$$\Phi_x = \Phi_{st} \left(\frac{\text{grad}_x}{\text{grad}_{st}} \right) \left(\frac{\eta_x^2}{\eta_{st}^2} \right) \quad (1)$$

Where the subscripts st and x denote standard and test respectively, Φ is the fluorescence quantum yield, grad refers to the gradient from the plot of integrated fluorescence intensity VS absorbance, and η is the refractive index of the solvent.

3. Results and Discussion

3.1 Synthesis and the formation mechanism of C-dots

In the present work, C-dots were prepared by a one-step thermal polymerization way directly using ethylene glycol as the sole carbon resource. With temperature increasing, the colorless solution changed to faint yellow gradually, suggesting the formation of C-dots. It is interesting that the pH of the solution was found to have obvious effect on the fluorescence of the obtained products. Fig. 1A shows the fluorescent emission spectra of the products synthesized from 2 ml ethylene glycol containing 0, 10, 20 mg NaOH and 1.5 ml HCl (1 M), respectively under the same experimental conditions. It can be seen that for the products synthesized from ethylene glycol with the absence of NaOH or with the presence of HCl, almost no fluorescence can be observed, suggesting no C-dots formation under such conditions. However, upon the addition of NaOH in ethylene glycol, the obtained products show strong fluorescence

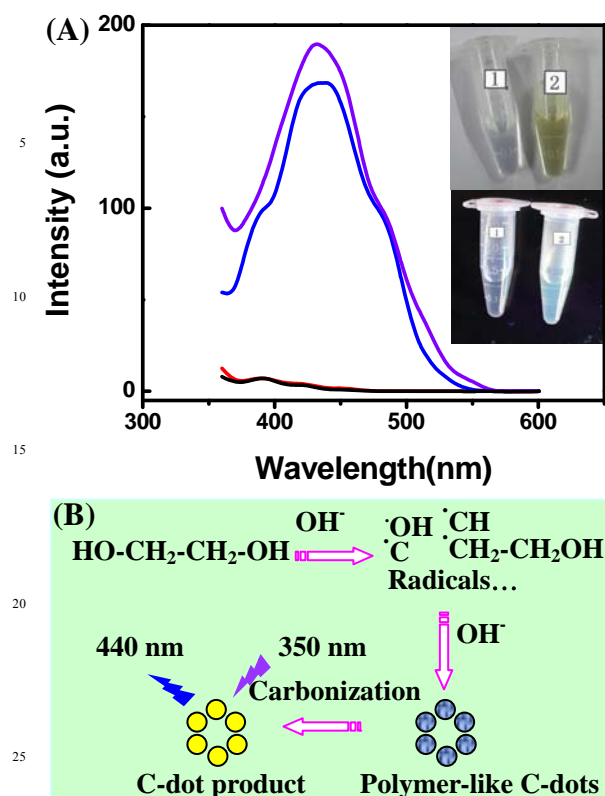


Fig. 1 (A) Fluorescent emission spectra of the products prepared from 2 ml ethyl glycol containing 1.5 ml 1 M HCl (black line), 0 mg NaOH (red line), 10 mg NaOH (green line), 20 mg NaOH (violet line) under the same experimental condition with an excitation at 350 nm. The insets show the digital photographs of the solutions of 2 ml ethyl glycol + 20 mg NaOH (number 1) and the corresponding C-dots product (number 2) under the irradiation of sunlight (top) and ultraviolet light (bottom). (B) Schematic representation of the formation of C-dots.

at 433 nm, indicating the production of C-dots, and the sample synthesized from solution with 20 mg NaOH exhibits the stronger fluorescence. The digital images in Fig. 1A inset compares the colors of the initial ethylene glycol (2 ml) + NaOH (20 mg) and the product under the daylight (top) and ultraviolet lamp (bottom) (number 1 and 2 represent the ethylene glycol and C-dots solutions, respectively). Obviously, different from the ethylene glycol solution, the product shows pale-yellow color under daylight lamp and exhibits a green color under the ultraviolet lamp. Note that further modification and purification steps are not needed in the preparation process, which makes the present synthesis method simple, distinctive and attractive for synthesis of fluorescent carbon nanodots. Importantly, addition of sodium hydroxide is a key factor for the formation of C-dots and the amount of NaOH has significant influence on the fluorescent intensity of the produced C-dots.

Here, the mechanism of the formation of carbon dots from ethylene glycol is proposed. We infer that the generation of radicals and carbonization at the elevated temperature result in the formation of C-dots, which is similar to the process and mechanism of electrochemical oxidation of low-molecular-weight alcohol that was reported earlier.²⁸ Overall, the formation

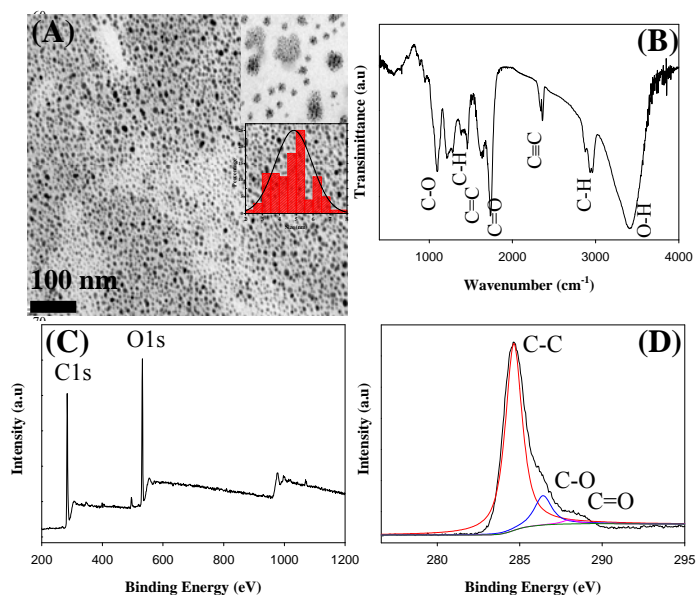


Fig. 2 (A) TEM image of the synthesized C-dots. Inset shows the magnified TEM image of the C-dot aggregations and the particle size distribution histogram. (B) Fourier-transformed infrared spectrum (FTIR) of the C-dots. (C) XPS survey spectrum of the as-synthesized C-dots. (D) XPS of the C1s spectrum.

process of carbon dots could be divided into three steps, as shown in Fig. 1B. Firstly, when the temperature rises to a certain value, the dehydration of the alcohol would occur and the chemical bonds of O-H, C-O, C-C in ethyl glycol could be broken, producing different kinds of radicals. In the following step, the active species could be self-assembled and crosslinked into different groups, and new chemical bonds could be formed to generate the polymer-like carbon dots. In the third step, the polymer-like carbon dots are finally carbonized into carbogenic C-dots through further dehydration between functional groups.¹⁹ It is noteworthy that the basic environment is very important for the preparation of the carbon dots as mentioned earlier. As discussed above, for ethyl glycol with the absence of sodium hydroxide or presence of hydrochloric acid, no C-dots were formed, which is consistent with the electrochemical-oxidation of alcohols in alkaline solution.²⁸⁻³² In this reaction system, the OH⁻ may act as the catalyst and evocator for the formation of C-dots. Moreover, the OH⁻ may also affect the surface state of C-dots as suggested by the discrepancy of fluorescence intensity. In the studies below, the C-dots prepared from ethyl glycol solution with 20 mg NaOH are used.

3.2 Characterization of the C-dots

Fig. 2A shows the typical transmission electron microscopy (TEM) images of the synthesized C-dots. At first sight of the TEM image, the deep black and large particles may come into notice. However, from the magnified TEM image shown in Fig. 2 inset (top), the large particles are actually the aggregates of C-dots. The aggregates show torispherical or flower-like morphology with a size in the range of 60–70 nm but without sediments in solution. Such observation suggests that the produced C-dots tend to aggregate into “C-dot clusters” in the

solution due to the hydrogen bonds or/and the affinity of the surface functional groups. According to the particle size distribution histogram calculated from one hundred of carbon dots (Fig. 2 inset, bottom), the carbon nanoparticles have a size distribution in 3~6 nm with an average size of 4.98 ± 1.5 nm.

Fig. 2B presents the Fourier-transformed infrared (FTIR) spectrum which reflects the surface functional groups of the obtained carbon dots. The peak at 3410 cm^{-1} could be assigned to the stretching vibration of O-H. The peaks at 2948 and 2880 cm^{-1} are attributed to the stretching vibrations of C-H, while the peak at 1449 cm^{-1} corresponds to the bending vibration of C-H. Besides the peaks at 2364 cm^{-1} originated from the stretching vibration of $\text{C}\equiv\text{C}$, the stretching vibrations of C-O can be identified by the peaks at 1221 and 1099 cm^{-1} . Moreover, the peaks at 1720 and 1615 cm^{-1} originate from the stretching modes of C=O and C=C, respectively. The FTIR spectrum together with the following XPS results indicate the successful preparation of C-dots with different kinds of surface chemical bonds such as C=C, $\text{C}\equiv\text{C}$, and surface functional groups such as -COOH, -OH which can enhance their water-solubility.

X-ray photoelectron spectroscopy (XPS) has been one of the frequently-used analytical techniques to analyze the valence states of the elements in carbon materials. The XPS survey spectrum shown in Fig. 2C gives two sharp-pointed peaks of graphitic C1s at ca.284 eV and O1s at ca.532 eV, illustrating the presence of O-rich groups on the surface of carbon frame. The abundant oxygen-containing groups endow the C-dots with good water solubility, which is favorable for the detection of metal ions in water. Fig. 2D shows the high resolution spectrum of C1s. The deconvoluted three peaks with the binding energies of 284.7, 286.7, and 288.2 eV can be respectively assigned to the C=C/C-C, C-O, C=O, which is well consistent with the previous studies on carbon materials, e.g. graphene oxide.³³ Based on above characterizations, aromatic rings, epoxy, alkoxy and carboxyl groups may exist in the as-synthesized carbon dots.

The absorption and photoluminescence properties of the as-synthesized C-dots were also examined. Fig. 3A presents the UV-vis absorption spectra and photoluminescent emission spectra of C-dots in three kinds of solvents, including ethylene glycol (EG), ethanol and water. In the absorption spectra, two sharp absorption peaks located at 205 and 256 nm and a shoulder peak at 223 nm can be observed from the C-dots EG and ethanol solution. However, the peak at 205 nm disappeared and the shoulder-peak at 223 nm became less pronounced when the C-dots were dispersed in water. Such solvent effect on the optical properties of carbon materials has also been observed in the previous study.³⁴ Correspondingly, the fluorescence intensity of C-dots is also dependent on the solvents and the fluorescent intensity in ethanol and EG is much higher than that in water. Here, the solvent-dependent absorption and fluorescence intensity indicate the polarity-sensitive properties of the C-dot fluorophores, suggesting the effect of the surrounding micro-environment on the excited state dipole moment or the electronic structure of the C-dots. Fig. 3B gives the fluorescent excitation and emission spectra of the carbon nanodots with the maximum values around 350 nm and 440 nm respectively. The large Stokes shift is attributed to the effect of the nearby polar solvent molecules on the excited dipole moment of the C-dots.³⁵ According to Eq.(1),

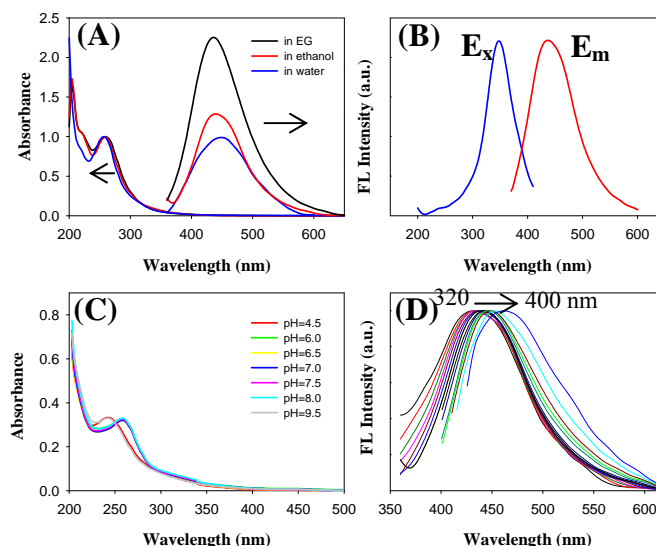


Fig. 3 (A) UV-vis absorption and the corresponding photoluminescent emission spectra ($\lambda_{\text{ex}} = 350$ nm) of the C-dots in ethyl glycol (EG, black lines), ethanol (red lines) and water (blue lines). (B) Fluorescent excitation and emission spectra of C-dots in water, $\lambda_{\text{ex}} = 350$ nm, $\lambda_{\text{em}} = 440$ nm. (C) UV-vis absorption spectra of the C-dot in different pH buffer solutions. (D) Photoluminescent emission spectra of the C-dots at different excitation wavelength from 320 to 400 nm.

the quantum yield of the C-dots was calculated to be 3.02 % by using quinine sulfate as a reference. Fig. 3C shows the influence of hydrogen ions on the optical absorption of the C-dots. There is the maximum absorption difference of 8 nm in the basic and acid buffer solutions, again reflecting the chemical microenvironmental effect on the surface state or molecule state of C-dots. The fluorescent emission under different excitation wavelength was also investigated. As shown in Fig. 3D, with the excitation wavelength changing from 320 to 400 nm, the maximum emission peak exhibits a red shift from 430 to 460 nm. Such excitation-dependent emission properties have been reported in the studies of carbon dots and graphene quantum dots, which could be ascribed to the different surface states of the prepared C-dots.³⁴

3.3 Sensitive and selective detection of Ag^+ ions based on the Ag^+ -induced fluorescence enhancement of C-dots

Fluorescent C-dots have been widely used for the detection of various metal ions based on the metal ions-induced fluorescence quenching. Interestingly, we found that the addition of Ag^+ ions into the present C-dot aqueous solution can enhance but not quench the fluorescence. Moreover, there is a linear relationship between the concentration of Ag^+ ions and the enhanced fluorescence intensity, based on which silver ions can be sensitively detected. To study the response rate of fluorescence signal of C-dots to Ag^+ ions, the required time for the reaction between C-dots and added Ag^+ ions was first evaluated by mixing C-dots with 35 μL , 10 mM Ag^+ in aqueous solution. Fig. S1 shows the time-dependent fluorescence of C-dots, it can be seen that the fluorescence intensity shows almost no change after 1 min. Therefore, in the following studies, each emission spectrum is recorded after 1 min of mixing C-dots and different concentrations of Ag^+ ions.

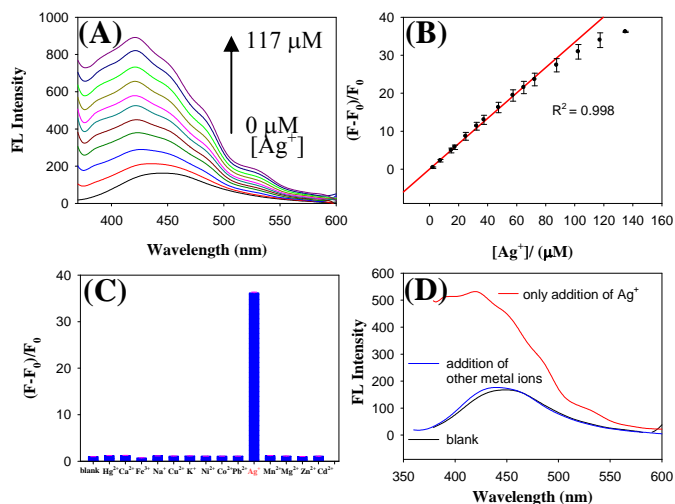


Fig. 4 (A) Fluorescent emission spectra of the C-dots aqueous solution with the addition of different concentrations of Ag^+ increasing from 0 to 117 μM , ($\lambda_{\text{ex}} = 350 \text{ nm}$). (B) Change of fluorescence intensity of the C-dots versus the Ag^+ concentration. (F and F_0 represent fluorescence intensities with the presence and absence of metal ions, respectively) (C) Fluorescence response of the C-dots aqueous solution to the addition of different metal ions with a concentration of 135 μM . (D) Fluorescent emission spectra of C-dots aqueous solution (black line), and the solution after adding 55 μM Ag^+ ions (red line) and all other metal ions (including Na^+ , K^+ , Ca^{2+} , Cu^{2+} , Mg^{2+} , Hg^{2+} , Zn^{2+} , Ni^{2+} , Co^{2+} , Cd^{2+} , Mn^{2+} , Pb^{2+} , blue line).

Fig. 4A displays the fluorescent emission spectra of C-dots upon addition of different concentrations of Ag^+ ions changing from 0 to 117 μM . Obviously, different from the usual quenching effect of metal ions on fluorescence of C-dots, the peak intensity of the emission increases with the concentration of Ag^+ ions increasing. Hence, the prepared C-dots can be used as probes for the fluorescence turn-on detection of Ag^+ . Meanwhile, the emission peak shows blue-shift from 440 nm to 425 nm. Fig. 4B displays the calibration curve for Ag^+ ions detection, which exhibits a good linearity in the concentration range from 0 to 90 μM with a correlation coefficient of 0.998 (F and F_0 correspond to the fluorescence intensities of the C-dots solution with the presence and absence of silver ions, respectively). It should be pointed out that the present linear range is much larger than those reported previously.^{7, 36} The linear regression can be expressed as: $F - F_0 / F_0 = 0.33218 * C_{\text{Ag}^+} - 0.30399$. The limit of detection (LOD) of Ag^+ ions in the present system was calculated to be 320 nM ($S/N=3$), which is much less than the concentration of Ag^+ ions in daily table-water (460 nM or 0.050 mg L^{-1}) determined by the US Environmental Protection Agency (EPA).³⁷

To assess the selectivity of the fluorescent C-dots for recognition of Ag^+ ions, the fluorescence intensities of the C-dots solution with the presence of different metal cations (i.e. Hg^{2+} , Ca^{2+} , Fe^{3+} , Na^+ , Cu^{2+} , K^+ , Ni^{2+} , Co^{2+} , Pb^{2+} , Mn^{2+} , Mg^{2+} , Zn^{2+} , Cd^{2+}) were measured. As shown in Fig. 4C, compared to the blank C-dots solution, enhanced fluorescence intensity was obtained for the C-dots solution containing 135 μM Ag^+ ions, whereas a negligible intensity change can be observed upon addition of other metal cations with the same concentration (135 μM). On the other hand, the interference of other metal ions on

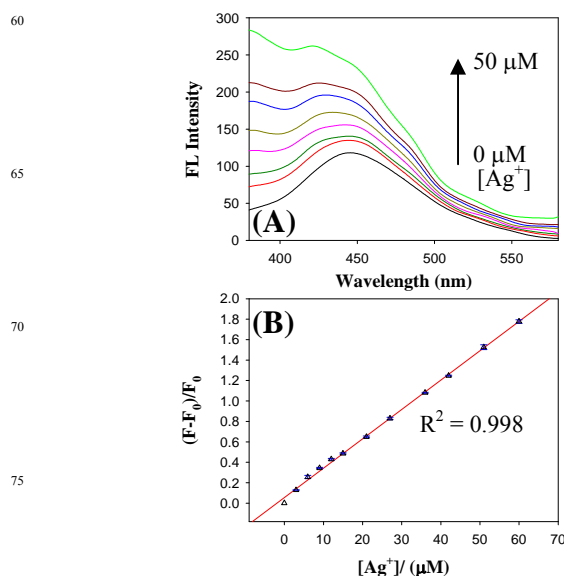


Fig. 5 (A) Fluorescent emission spectra of the C-dots with the presence of different concentrations of Ag^+ from 0 to 50 μM in lake water, ($\lambda_{\text{ex}} = 350 \text{ nm}$). (B) The relationship between $(F - F_0) / F_0$ and Ag^+ concentration.

the detection of Ag^+ was also examined. From Fig. 4D, one can see that the fluorescence intensity of C-dots solution can be largely enhanced by adding only 55 μM Ag^+ (red line). However, the addition of the same concentration of all other metal ions (blue line) can result in almost no change of the fluorescence intensity. These results indicate that the prepared C-dots have high sensitivity and selectivity for Ag^+ detection by taking advantage of its unique enhancement effect on the fluorescence of C-dots.

Furthermore, the application of the carbon nanofluorophore for the sensing of Ag^+ in real environmental water can also be achieved. Before the experiment for Ag^+ detection, the lake water was first filtered by a 0.22 μm membrane and then centrifuged at 10000 rpm for 10 min to remove the large and insoluble impurities. Fig. 5A shows the changes of fluorescent emission spectra of C-dots in lake water containing different concentrations of Ag^+ . From the corresponding calibration curve of $(F - F_0) / F_0$ vs the concentration of Ag^+ within the range from 0 μM to 50 μM in lake water, it can be seen clearly that the fluorescence intensity shows a good linearity over the concentration of Ag^+ ions. Note that although there are all kinds of impurities such as minerals and organics in the real lake water, the as-prepared carbon dots is still sensitive to Ag^+ concentration, indicating the promising application of the C-dots in detecting Ag^+ in real environmental sample. It should be pointed out that because the original concentration of Ag^+ in the lake water sample is much lower than the LOD, the present sensing system did not give the reasonable concentration of silver ions, which is consistent with the result from ICP-MS measurement (didn't give the certain value).

Compared to the previously reported methods for detection of Ag^+ ions, e.g. sensing systems based on deoxyribonucleic acid, gold clusters, gold nanoparticles,^{7, 36, 38, 39} the low cost and high selectivity (without masking agent) of the present C-dots is more attracting and would be more suitable for the real application.

Cite this: DOI: 10.1039/c0xx00000x

www.rsc.org/xxxxxx

ARTICLE TYPE

Table 1 Comparison of Detection Performance of Different Fluorescent Probes for Ag⁺ Detection

Detection probes	Detection mechanism	Detection Limit	Linear range	Reference
GO-oligonucleotide	Fluorescence enhancement	5 nM	/	7
Au nanoclusters	Fluorescence enhancement	62 nM	25 nM-3 μM	36
DNA-SWCNT	Fluorescence enhancement	1 nM	0-150 nM	38
Au nanoparticles	LSPR light scatter	62 nM	0.13-1.12 μM	39
Graphene quantum dots	Fluorescence quenching	0.3 mM	/	40
N-doped C-dots	Fluorescence enhancement	1 μM	1-100 μM	41
C-dots	Fluorescence quenching	0.13 μM	0.5-6 μM	42
C-dots	Fluorescence enhancement	320 nM	0-90 μM	This work

10 Meanwhile, compared to the reported graphene quantum dots and other C-dots,⁴⁰⁻⁴² the present work presents a simpler one-step synthesis and wider linear range for Ag⁺ detection. Table 1 summarizes the sensing performances of different fluorescent probes for Ag⁺ detection. We believe this work provides an alternative convenient platform for the detection of silver ions and new insights into the fluorescence enhancing mechanism (discussed below).

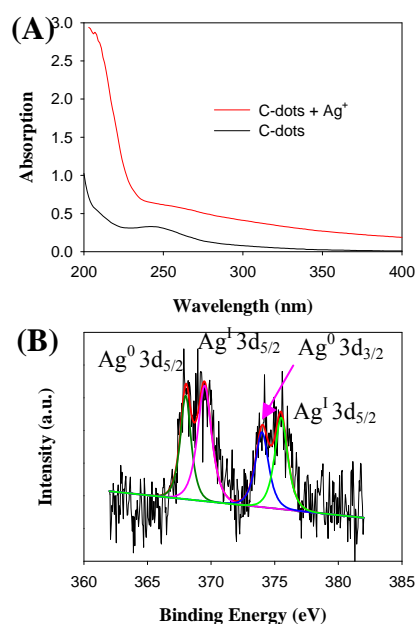
3.4 Fluorescence enhancing mechanism

20 It is widely accepted that the photoluminescence of carbon dots arises from the radiative combination of the trapped surface holes and electrons.⁴³ In this study, the fluorescence enhancement of C-dots induced by silver ions may be ascribed to the metal-enhanced fluorescence mechanism, i.e. the produced Ag nanocluster could increase the local incident field of the C-dots.³⁵ It is well known that enhanced fluorescence of some fluorophores would be induced by metals, such as silver and gold.⁴⁴ From Table 2, we can quickly find that the reduction potential of silver (I)/silver is much higher than other metal ions except for Hg²⁺/Hg.³⁰ Thus, we can propose the following mechanism. Upon addition of Ag⁺ into the C-dots solution, the oxidation-reduction reaction would occur on the surface of C-dots, i.e. Ag⁺ is reduced to metal Ag⁰ while C-dots is oxidized. The interaction between C-dots and the formed tiny silver nanoclusters could enhance the radiative emission of C-dots.⁴⁵ Since the formed Ag nanoclusters can not be separated from the C-dots, it is not clear whether there is fluorescence contribution from the Ag nanoclusters or not. However, the present Ag nanoclusters are not covered by organic ligands, their fluorescence should be different from the reported fluorescent monolayer-protected metal clusters.⁴⁶⁻⁴⁹ The detailed fluorescence enhancement mechanism needs to be further studied. On the other hand, metal nanoparticles or nanoclusters in situ formed on carbon materials have been reported previously, such as Ag nanoclusters on carbon nanodots,⁵⁰ Ag nanoparticles on cysteine,⁵¹ Pd nanoparticles on carbon nanodots,⁵² and Au and Pt nanoparticles on carbon nanotubes⁵³ etc. Here, from the UV-vis absorption comparison shown in Fig. 6A, after the addition of

Table 2 Standard electrode potentials in aqueous solution at 25 °C (vs NHE)^a

Metal ion	Potential (V)	Metal ion	Potential (V)
K ⁺ /K	-2.925	Cd ²⁺ /Cd	-0.4025
Ca ²⁺ /Ca	-2.84	Co ²⁺ /Co	-0.277
Na ⁺ /Na	-2.714	Ni ²⁺ /Ni	-0.257
Mg ²⁺ /Mg	-2.356	Pb ²⁺ /Pb	-0.1251
Mn ²⁺ /Mn	-1.180	Cu ²⁺ /Cu	0.340
Fe ³⁺ /Fe	-0.037	Hg ²⁺ /Hg	0.851
Zn ²⁺ /Zn	-0.7626	Ag ⁺ /Ag	0.7991

^aThe data in this Table are taken from A. J. Bard, L. R. Faulkner, Eds., "Electrochemical Methods Fundamentals and Applications, 2nd.", John Wiley & Sons, Inc.



75 **Fig. 6** (A) UV-vis absorption spectra of C-dots with and without the addition of Ag⁺ ions (C_{Ag^+} in water is 35 μM). (B) XPS spectrum of the C-dots solution after addition of Ag⁺ ions.

Ag⁺ into the C-dots solution, the surface plasmon resonance of the produced Ag clusters can effectively improve the light absorption. Also from the XPS result in Fig. 6B, both Ag⁺ (Ag 3d_{5/2}, 369.47 eV; Ag 3d_{3/2}, 375.54 eV) and Ag⁰ (Ag 3d_{5/2}, 367.9 eV; Ag 3d_{3/2}, 374.05 eV) are present in the solution. It is noteworthy that due to the electronic interaction between metallic Ag and C-dots, the binding energy of Ag 3d shows a little downshift compared to that of bulk Ag (368.5 eV; 374.3 eV). On the other hand, it is well known that Hg²⁺ is heavy ion and its bulk metal (Hg⁰) is not easy to produce plasmonic properties which are the basic requirements for metal-enhanced fluorescence.⁵⁴ Therefore, Hg²⁺ ions didn't exhibit enhancement effect on the fluorescence of C-dots. In the previous studies,^{55,56} it was found that the metal-enhanced fluorescence depends on the distance between metal nanoparticles and fluorescein. Usually, the larger separation distance between fluorescein and metal surface are considered to be more favorable for the fluorescence enhancement. However, the exact distance for fluorescence enhancement is still unknown. Moreover, the fluorescence enhancement is strongly affected by chemical environments and fluorescent systems. Further studies are still needed to well understand the fluorescence enhancing mechanism of nanocluster systems.

4. Conclusion

In summary, we successfully synthesized luminescent C-dots through a simple, low-cost and environmentally friendly process by using ordinary ethyl glycol as carbon source. The prepared C-dots showed excitation-dependent blue fluorescent emission in aqueous solution. Based on our proposed mechanism, silver ions could be reduced to Ag⁰ clusters on the surface of the C-dots, which can enhance efficiently the fluorescence intensity of the C-dots. To the best of our knowledge, the metal ions-induced enhancement effect on fluorescence of C-dots has been rarely reported. More importantly, the enhanced fluorescence intensity exhibited a good linearity on the concentration of Ag ions in aqueous solution. Therefore, the C-dots can be used as fluorescence turn-on probes for detection of Ag⁺ ions in water with high sensitivity and selectivity.

Acknowledgements

This work was supported by the National Natural Science Foundation of China (No. 21275136) and the Natural Science Foundation of Jilin province, China (No. 201215090).

Notes and references

^a State Key Laboratory of Electroanalytical Chemistry, Changchun Institute of Applied Chemistry, Chinese Academy of Sciences, Changchun 130022, Jilin, China. Tel: +86431-85262723; E-mail: weichen@ciac.ac.cn
^b University of Chinese Academy of Sciences, Beijing 100039, China
 † Electronic Supplementary Information (ESI) available: Dependence of fluorescence intensity of C-dots on the mixing time. See DOI: 10.1039/b000000x/

1. W. de Vries, P. F. A. M. Romkens and G. Schutze, *Rev. Environ. Contam. T.*, 2007, **191**, 91-130.
 2. H. T. Ratte, *Environ. Toxicol. Chem.*, 1999, **18**, 89-108.

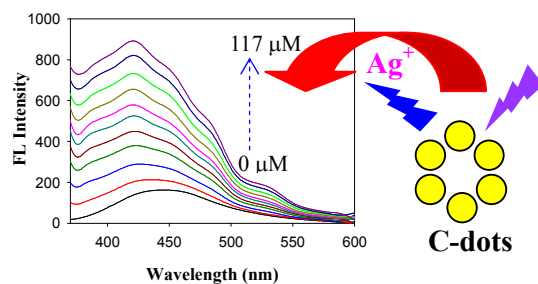
3. P. Doudoroff and M. Katz, *Sewage and Industrial Wastes*, 1953, 802-839.
4. G. S. Reddi and C. R. M. Rao, *Analyst*, 1999, **124**, 1531-1540.
5. A. Chatterjee, M. Santra, N. Won, S. Kim, J. K. Kim, S. Bin Kim and K. H. Ahn, *J. Am. Chem. Soc.*, 2009, **131**, 2040-2041.
6. R. H. Yang, W. H. Chan, A. W. M. Lee, P. F. Xia, H. K. Zhang and K. A. Li, *J. Am. Chem. Soc.*, 2003, **125**, 2884-2885.
7. Y. Q. Wen, F. F. Xing, S. J. He, S. P. Song, L. H. Wang, Y. T. Long, D. Li and C. H. Fan, *Chem. Commun.*, 2010, **46**, 2596-2598.
8. E. M. Nolan and S. J. Lippard, *J. Am. Chem. Soc.*, 2003, **125**, 14270-14271.
9. J. Panchompoo, L. Aldous, M. Baker, M. I. Wallace and R. G. Compton, *Analyst*, 2012, **137**, 2054-2062.
10. Y. X. Fang, S. J. Guo, D. Li, C. Z. Zhu, W. Ren, S. J. Dong and E. K. Wang, *ACS Nano*, 2012, **6**, 400-409.
11. Q. Liu, B. D. Guo, Z. Y. Rao, B. H. Zhang and J. R. Gong, *Nano Lett.*, 2013, **13**, 2436-2441.
12. J. Ju, R. Z. Zhang, S. J. He and W. Chen, *RSC Adv.*, 2014, **4**, 52583-52589.
13. A. Jaiswal, S. S. Ghosh and A. Chattopadhyay, *Chem. Commun.*, 2012, **48**, 407-409.
14. C. Q. Ding, A. W. Zhu and Y. Tian, *Accounts Chem. Res.*, 2014, **47**, 20-30.
15. M. Zheng, Z. G. Xie, D. Qu, D. Li, P. Du, X. B. Jing and Z. C. Sun, *ACS Appl. Mater. Inter.*, 2013, **5**, 13242-13247.
16. A. Prasanna and T. Imae, *Ind. Eng. Chem. Res.*, 2013, **52**, 15673-15678.
17. S. Gomez-de Pedro, A. Salinas-Castillo, M. Ariza-Avidad, A. Lapresta-Fernandez, C. Sanchez-Gonzalez, C. S. Martinez-Cisneros, M. Puyol, L. F. Capitan-Vallvey and J. Alonso-Chamarro, *Nanoscale*, 2014, **6**, 6018-6024.
18. R. Zhang and W. Chen, *Biosens. Bioelectron.*, 2014, **55**, 83-90.
19. S. J. Zhu, Q. N. Meng, L. Wang, J. H. Zhang, Y. B. Song, H. Jin, K. Zhang, H. C. Sun, H. Y. Wang and B. Yang, *Angew. Chem. Int. Edit.*, 2013, **52**, 3953-3957.
20. Y. Q. Dong, R. X. Wang, G. L. Li, C. Q. Chen, Y. W. Chi and G. N. Chen, *Anal. Chem.*, 2012, **84**, 6220-6224.
21. H. M. R. Goncalves, A. J. Duarte and J. C. G. E. da Silva, *Biosens. Bioelectron.*, 2010, **26**, 1302-1306.
22. H. Zhang, Y. Chen, M. Liang, L. Xu, S. Qi, H. Chen and X. Chen, *Anal. Chem.*, 2014, **86**, 9846-9852.
23. Y. F. Wang and A. G. Hu, *J. Mater. Chem. C*, 2014, **2**, 6921-6939.
24. J. H. Shen, Y. H. Zhu, X. L. Yang and C. Z. Li, *Chem. Commun.*, 2012, **48**, 3686-3699.
25. L. L. Li, G. H. Wu, G. H. Yang, J. Peng, J. W. Zhao and J. J. Zhu, *Nanoscale*, 2013, **5**, 4015-4039.
26. J. Ju and W. Chen, *Biosens. Bioelectron.*, 2014, **58**, 219-225.
27. M. Algarra, B. B. Campos, K. Radotic, D. Mutavdzic, T. Badosz, J. Jimenez-Jimenez, E. Rodriguez-Castellon and J. C. G. E. da Silva, *J. Mater. Chem. A*, 2014, **2**, 8342-8351.
28. J. Deng, Q. Lu, N. Mi, H. Li, M. Liu, M. Xu, L. Tan, Q. Xie, Y. Zhang and S. Yao, *Chem.-Eur. J.*, 2014, **20**, 4993-4999.
29. G. Sundholm, *J. Electroanal. Chem. Interfac. Electrochem.*, 1971, **31**, 265-267.
30. S. Raicheva, S. Kalcheva, M. Christov and E. Sokolova, *J. Electroanal. Chem. Interfac. Electrochem.*, 1974, **55**, 213-222.
31. J. Steven, *Chem. Commun.*, 1965, **273**.
32. W. Dixon and R. Norman, *J. Chem. Soc.*, 1963, 3119-3120.
33. Y. Z. Lu, Y. Y. Jiang, W. T. Wei, H. B. Wu, M. M. Liu, L. Niu and W. Chen, *J. Mater. Chem.*, 2012, **22**, 2929-2934.
34. X. J. Mao, H. Z. Zheng, Y. J. Long, J. Du, J. Y. Hao, L. L. Wang and D. B. Zhou, *Spectrochim. Acta. A*, 2010, **75**, 553-557.
35. C. D. Geddes and J. R. Lakowicz, *J. Fluoresc.*, 2002, **12**, 121-129.
36. J. Sun, Y. Yue, P. Wang, H. L. He and Y. D. Jin, *J. Mater. Chem. C*, 2013, **1**, 908-913.
37. United States Environmental Protection Agency, Washington DC 440/5-80-071, 1980.
38. C. Zhao, K. G. Qu, Y. J. Song, C. Xu, J. S. Ren and X. G. Qu, *Chem.-Eur. J.*, 2010, **16**, 8147-8154.
39. C. K. Wu, C. Xiong, L. J. Wang, C. C. Lan and L. S. Ling, *Analyst*, 2010, **135**, 2682-2687.

40. A. Suryawanshi, M. Biswal, D. Mhamane, R. Gokhale, S. Patil, D. Guin and S. Ogale, *Nanoscale*, 2014, **6**, 11664-11670.
41. Z. S. Qian, J. J. Ma, X. Y. Shan, H. Feng, L. X. Shao and J. R. Chen, *Chem.-Eur. J.*, 2014, **20**, 2254-2263.
- 5 42. L. M. Shen, M. L. Chen, L. L. Hu, X. W. Chen and J. H. Wang, *Langmuir*, 2013, **29**, 16135-16140.
43. X. Wang, L. Cao, F. S. Lu, M. J. Mezziani, H. Li, G. Qi, B. Zhou, B. A. Harruff, F. Kermarrec and Y. P. Sun, *Chem. Commun.*, 2009, 3774-3776.
- 10 44. C. Y. Li, Y. H. Zhu, X. Q. Zhang, X. L. Yang and C. Z. Li, *RSC Adv.*, 2012, **2**, 1765-1768.
45. Z. K. Wu, M. Wang, J. Yang, X. H. Zheng, W. P. Cai, G. W. Meng, H. F. Qian, H. M. Wang and R. C. Jin, *Small*, 2012, **8**, 2028-2035.
46. X. Yuan, B. Zhang, Z. T. Luo, Q. F. Yao, D. T. Leong, N. Yan and J. P. Xie, *Angew. Chem. Int. Edit.*, 2014, **53**, 4623-4627.
- 15 47. Z. T. Luo, X. Yuan, Y. Yu, Q. B. Zhang, D. T. Leong, J. Y. Lee and J. P. Xie, *J. Am. Chem. Soc.*, 2012, **134**, 16662-16670.
48. Y. Yu, Z. T. Luo, D. M. Chevrier, D. T. Leong, P. Zhang, D. E. Jiang and J. P. Xie, *J. Am. Chem. Soc.*, 2014, **136**, 1246-1249.
- 20 49. Z. T. Luo, V. Nachammai, B. Zhang, N. Yan, D. T. Leong, D. E. Jiang and J. P. Xie, *J. Am. Chem. Soc.*, 2014, **136**, 10577-10580.
50. M. M. Liu and W. Chen, *Nanoscale*, 2013, **5**, 12558-12564.
51. H. L. Liu, Y. J. Ye, J. Chen, D. Y. Lin, Z. Jiang, Z. J. Liu, B. Sun, L. B. Yang and J. H. Liu, *Chem.-Eur. J.*, 2012, **18**, 8037-8041.
- 25 52. W. T. Wei and W. Chen, *J. Power Sources*, 2012, **204**, 85-88.
53. H. C. Choi, M. Shim, S. Bangsaruntip and H. J. Dai, *J. Am. Chem. Soc.*, 2002, **124**, 9058-9059.
54. Y. X. Zhang, H. Goncalves, J. C. G. E. da Silva and C. D. Geddes, *Chem. Commun.*, 2011, **47**, 5313-5315.
- 30 55. L. T. Kong, J. Wang, G. C. Zheng and J. H. Liu, *Chem. Commun.*, 2011, **47**, 10389-10391.
56. G. L. Wang, H. J. Jiao, X. Y. Zhu, Y. M. Dong and Z. J. Li, *Analyst*, 2013, **138**, 2000-2006.

35

One-Pot Synthesis of Carbon Nanodots for Fluorescence Turn-on Detection of Ag^+ based on the Ag^+ -Induced Enhancement of Fluorescence

Xiaohui Gao,^{a,b} Yizhong Lu,^{a,b} Ruizhong Zhang,^{a,b} Shuijian He,^{a,b} Jian Ju,^a Minmin Liu,^{a,b} Lei Li,^a Wei Chen^{*,a}



Fluorescent carbon dots prepared by a heat treatment of ethyl glycol solution can serve as fluorescence turn-on probes for sensitive and selective detection of Ag^+ ions